OPEN ACCESS Freely available online

PLoS one

# $G\alpha_{i2}$- and $G\alpha_{i3}$-Specific Regulation of Voltage-Dependent L-Type Calcium Channels in Cardiomyocytes

**Sara Dizayee[1], Sonja Kaestner[1], Fabian Kuck[2], Peter Hein[1], Christoph Klein[1], Roland P. Piekorz[2], Janos Meszaros[1], Jan Matthes[1], Bernd Nürnberg[2,3], Stefan Herzig[1]***

**1** Department of Pharmacology, University of Cologne, Cologne, Germany, **2** Department of Biochemistry and Molecular Biology II, University Hospital and Clinics, University of Düsseldorf, Düsseldorf, Germany, **3** Department of Pharmacology and Toxicology, Interfaculty Center of Pharmacogenomics and Pharmaceutical Research, University of Tübingen, Tübingen, Germany

## Abstract

***Background:*** Two pertussis toxin sensitive $G_i$ proteins, $G_{i2}$ and $G_{i3}$, are expressed in cardiomyocytes and upregulated in heart failure. It has been proposed that the highly homologous $G_i$ isoforms are functionally distinct. To test for isoform-specific functions of $G_i$ proteins, we examined their role in the regulation of cardiac L-type voltage-dependent calcium channels (L-VDCC).

***Methods:*** Ventricular tissues and isolated myocytes were obtained from mice with targeted deletion of either $G\alpha_{i2}$ ($G\alpha_{i2}^{-/-}$) or $G\alpha_{i3}$ ($G\alpha_{i3}^{-/-}$). mRNA levels of $G\alpha_{i/o}$ isoforms and L-VDCC subunits were quantified by real-time PCR. $G\alpha_i$ and $Ca_v\alpha_1$ protein levels as well as protein kinase B/Akt and extracellular signal-regulated kinases 1/2 (ERK1/2) phosphorylation levels were assessed by immunoblot analysis. L-VDCC function was assessed by whole-cell and single-channel current recordings.

***Results:*** In cardiac tissue from $G\alpha_{i2}^{-/-}$ mice, $G\alpha_{i3}$ mRNA and protein expression was upregulated to 187±21% and 567±59%, respectively. In $G\alpha_{i3}^{-/-}$ mouse hearts, $G\alpha_{i2}$ mRNA (127±5%) and protein (131±10%) levels were slightly enhanced. Interestingly, L-VDCC current density in cardiomyocytes from $G\alpha_{i2}^{-/-}$ mice was lowered (−7.9±0.6 pA/pF, n = 11, $p<0.05$) compared to wild-type cells (−10.7±0.5 pA/pF, n = 22), whereas it was increased in myocytes from $G\alpha_{i3}^{-/-}$ mice (−14.3±0.8 pA/pF, n = 14, $p<0.05$). Steady-state inactivation was shifted to negative potentials, and recovery kinetics slowed in the absence of $G\alpha_{i2}$ (but not of $G\alpha_{i3}$) and following treatment with pertussis toxin in $G\alpha_{i3}^{-/-}$. The pore forming $Ca_v\alpha_1$ protein level was unchanged in all mouse models analyzed, similar to mRNA levels of $Ca_v\alpha_1$ and $Ca_v\beta_2$ subunits. Interestingly, at the cellular signalling level, phosphorylation assays revealed abolished carbachol-triggered activation of ERK1/2 in mice lacking $G\alpha_{i2}$.

***Conclusion:*** Our data provide novel evidence for an isoform-specific modulation of L-VDCC by $G\alpha_i$ proteins. In particular, loss of $G\alpha_{i2}$ is reflected by alterations in channel kinetics and likely involves an impairment of the ERK1/2 signalling pathway.

**Citation:** Dizayee S, Kaestner S, Kuck F, Hein P, Klein C, et al. (2011) $G\alpha_{i2}$- and $G\alpha_{i3}$-Specific Regulation of Voltage-Dependent L-Type Calcium Channels in Cardiomyocytes. PLoS ONE 6(9): e24979. doi:10.1371/journal.pone.0024979

**Editor:** Vladimir E. Bondarenko, Georgia State University, United States of America

**Received** May 19, 2011; **Accepted** August 23, 2011; **Published** September 26, 2011



**Funding:** This study was supported by Deutsche Forschungsgemeinschaft (DFG), He 1578/13-1 and 2 to Dr. Herzig. Work in the lab of Dr. Piekorz and Dr. Nürnberg was supported by DFG (SFB 612) and the Forschungskommission der Medizinischen Fakultät der HHU Düsseldorf. The funders had no role in study design, data collection and analysis, decision to publish, or preparation of the manuscript.

**Competing Interests:** The authors have declared that no competing interests exist.

* E-mail: stefan.herzig@uni-koeln.de

## Introduction

G protein-mediated signalling plays a central role in regulation of cardiomyocyte function. Heterotrimeric G proteins consist of three subunits, Gα, Gβ, and Gγ. Agonist-occupied receptors induce dissociation of GDP from and binding of GTP to the G protein α subunit, resulting in G protein activation. Activated Gα and Gβγ subunits couple to a plethora of effectors, including enzymes and ion channels, and hence are involved in many regulatory processes [1,2]. The role of stimulatory $G_s$ and inhibitory $G_i$ proteins in cardiac signalling pathways is well studied [3,4]. Alterations of $G\alpha_i$ protein expression levels are found in heart disease [5], and heart failure in humans leads to upregulation of $G\alpha_{i2}$ and $G\alpha_{i3}$ [6,7,8,9]. Whether the upregulation of $G\alpha_{i2}$ and $G\alpha_{i3}$ in cardiomyocytes is causative, adaptive, or maladaptive still remains unclear.

Cardiac calcium channels are key components in complex signal transduction pathways and play an essential role in cardiac excitability and in coupling excitation to contraction [10]. One major pathway regulating calcium channels is mediated *via* G protein-mediated signalling. In the heart, the main sarcolemmal calcium channel is the voltage-dependent L-type calcium channel (L-VDCC). This channel is composed of three different subunits. The $\alpha_1$ subunit represents the pore forming subunit which contains the voltage sensor and the binding sites for calcium channel modulators [11]. It associates with two auxiliary subunits, β, and $\alpha_2\delta$ [12]. The functional properties of the pore forming subunit are differentially modified due to interaction with various β subunit isoforms [13,14,15,16]. Furthermore, receptor activated $G\alpha_s$ protein stimulates L-VDCCs via adenylyl cyclase-mediated increases in cAMP levels and protein kinase A (PKA) activity [3].

Activation of $G_i$ or $G_o$ modifies channel function *via* diverse signal cascades [17]. Thus, G protein signalling pathways are crucial in determining and balancing cardiomyocyte function *in vivo*.

In a previous study we addressed the role of $G\alpha_{i2}$ in $\beta_2$-adrenergic receptor-mediated signalling. Gene deletion of $G\alpha_{i2}$ in mice reduced single L-VDCC activity in $\beta_2$-adrenergic receptor-transgenic mice [18], whereas pertussis toxin (PTX) treatment reversed this effect. We speculated that this unexpected effect of PTX may have been caused by inhibiting an upregulated $G\alpha_{i3}$. Recently, Zuberi et al. [19] showed that $G\alpha_{i2}$ knockout leads to increased L-VDCC mRNA expression and a propensity towards ventricular arrhythmia. Muscarinic receptor-mediated inhibition of L-VDCC activity has been reported to depend on $G\alpha_{i2}$ but not $G\alpha_{i3}$ [20]. Though strongly suggested by these data, subtype-specific effects on cardiac L-VDCC by the highly homologous $G\alpha_{i2}$ and $G\alpha_{i3}$ isoforms remain unclear so far. Therefore, the present work was undertaken to elucidate whether the effects of these $G\alpha_i$ proteins are redundant or distinct. Using cardiomyocytes from mice lacking $G\alpha_{i2}$ or $G\alpha_{i3}$ and wild-type (WT) control animals, we determined structural and functional changes. Further, we examined specific signalling pathways implicated in cardiac L-VDCC modulation by $G\alpha_i$ protein. In this work, we provide evidence that the L-VDCC activity and kinetics are regulated in a non-redundant manner and we support this idea by demonstrating subtype-specific activation of the extracellular signal-regulated kinases 1/2 (ERK1/2) signalling cascade.

## Results

### $G\alpha_{i2}$ deficiency decreases, while $G\alpha_{i3}$ deficiency increases L-VDCC current density

To assess consequences of selective deletion of $G\alpha_{i2}$ or $G\alpha_{i3}$ genes, we measured whole-cell L-VDCC currents in cardiomyocytes from WT, $G\alpha_{i2}^{-/-}$, and $G\alpha_{i3}^{-/-}$ mice. Currents recorded at different test potentials are shown as representative original recordings and current-voltage diagrams of summarized data in Fig. 1A and B, respectively. In cardiomyocytes of $G\alpha_{i2}^{-/-}$ mice, the calcium current density at 0 mV was slightly but significantly reduced ($-7.9\pm0.6$ pA/pF, $n=11$, $p<0.05$) compared to WT ($-10.7\pm0.5$ pA/pF, $n=22$). In contrast, current density in cardiomyocytes from $G\alpha_{i3}^{-/-}$ mice was increased (to $-14.3\pm0.8$ pA/pF, $n=14$, $p<0.05$ vs. WT). Of note, the peak current in $G\alpha_{i2}^{-/-}$ cardiomyocytes is shifted towards higher voltages. Comparison of time-dependent inactivation by fitting revealed no alterations of fast and slow time constants in all genotypes (e.g. at 0 mV, $\tau_{fast}$: WT = $18.4\pm1.0$ ms, $G\alpha_{i2}^{-/-}$ = $26.9\pm4.0$ ms and $G\alpha_{i3}^{-/-}$ = $15.1\pm2.1$ ms; $\tau_{slow}$: WT = $95.3\pm4.2$ ms, $G\alpha_{i2}^{-/-}$ = $97.5\pm17$ ms and $G\alpha_{i3}^{-/-}$ = $94.9\pm9.9$ ms; n = 10–13). To test whether changes in

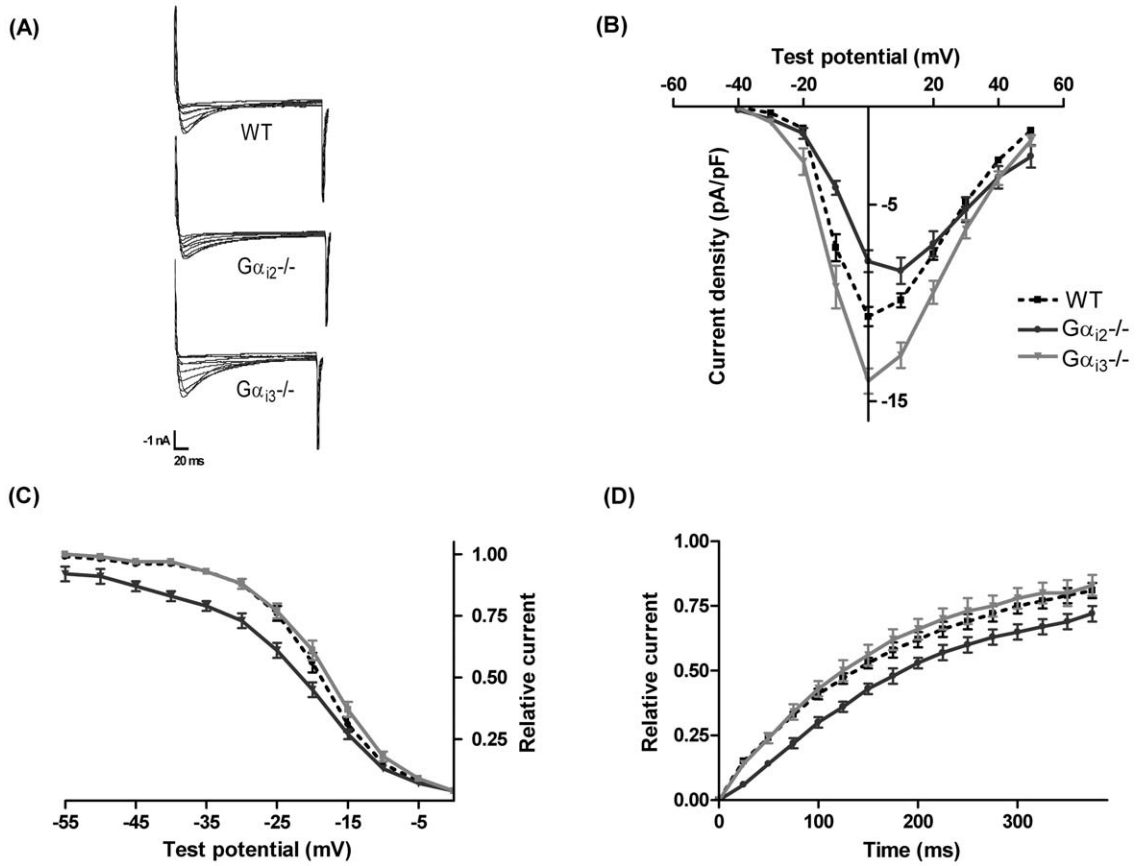


**Figure 1. Cardiac whole-cell L-type calcium currents.** Representative original current traces obtained at different test potentials (A) and IV-curves (B) reveal an increase of calcium current in ventricular myocytes from mice lacking $G\alpha_{i3}$ and a decrease in mice lacking $G\alpha_{i2}$ as compared to WT mice. (C) Steady-state inactivation of $G\alpha_{i2}^{-/-}$ ($n=11$) is shifted to more negative voltages as compared to $G\alpha_{i3}^{-/-}$ ($n=13$, $p<0.05$) and WT ($n=18$, $p<0.05$). (D) A slowing of the recovery time constant $\tau$ is found in cardiomyocytes from $G\alpha_{i2}^{-/-}$ mice ($287\pm21$ ms, $n=9$) as compared to $G\alpha_{i3}^{-/-}$ cells ($n=9$) and WT ($n=16$).
doi:10.1371/journal.pone.0024979.g001

gating account for the observed differences in current density, we examined kinetic and steady state properties of activation and inactivation.

## L-VDCC kinetics are altered by $G\alpha_{i2}$ deletion, but not by $G\alpha_{i3}$ deletion

The steady-state inactivation properties (Fig. 1C) in $G\alpha_{i2}^{-/-}$ cardiomyocytes were altered compared to WT cells as reflected by a significant leftward shift of $V_{0.5}$ ($G\alpha_{i2}^{-/-}$: $-23.4\pm1.0$ mV, n = 11, WT: $-19.2\pm0.7$ mV, n = 18) and an increased slope factor (Table 1). In addition, recovery from inactivation was slowed in cardiomyocytes from mice lacking $G\alpha_{i2}$ ($\tau$: $287\pm21$ ms, n = 9, $p<0.05$) in comparison to WT animals ($\tau$: $215\pm14$ ms, n = 16; Fig. 1D). In contrast, whole-cell currents in cells form $G\alpha_{i3}^{-/-}$ mice were indistinguishable from WT regarding both steady state inactivation ($V_{0.5}$: $-18.2\pm0.9$ mV, n = 13, Table 1) and recovery from inactivation ($\tau$: $203\pm24$ ms, n = 9). Thus, currents from $G\alpha_{i2}^{-/-}$ mice show altered kinetic properties and this might explain the decreased current density described above (Fig. 1). Despite increased current density no alteration of current kinetics in $G\alpha_{i3}^{-/-}$ myocytes was visible. Thus we analyzed single-channel activity to elucidate the opposing effects seen on whole-cell currents in $G\alpha_{i2}^{-/-}$ and $G\alpha_{i3}^{-/-}$ cardiomyocytes.

## No major changes in gating properties of single L-VDCC in $G\alpha_{i3}^{-/-}$ cardiomyocytes

Single-channel current recordings in $G\alpha_{i3}^{-/-}$ cardiomyocytes revealed a trend towards increased peak ensemble average currents (Fig. 2B) and higher open probability (Fig. 2C) when compared to WT cardiomyocytes (Table 2). These effects are based on a significant reduction of the mean closed time ($3.8\pm0.5$ ms vs. $6.6\pm0.9$ ms, n = 6–7, $p<0.05$; Fig. 2D). Together with a significantly decreased slow time constant of the closed state and by trend a reduced first latency (Table 2) our single-channel data suggest that in $G\alpha_{i3}^{-/-}$ exit from deeper closed states of L-VDCC is facilitated. Given that single-channel activity in $G\alpha_{i2}^{-/-}$ mice was decreased by trend [18] our findings presented here suggest that $G\alpha_{i2}^{-/-}$ or $G\alpha_{i3}^{-/-}$ knockout leads to distinct changes of cardiac L-VDCC properties. Yet, these only slight functional changes alone do not elucidate the more remarkable augmentation of calcium current density in $G\alpha_{i3}^{-/-}$. Since the remaining $G\alpha_i$ isoform might have compensated for effects of $G\alpha_{i3}$ deficiency we next checked the expression levels of $G\alpha_{i2}$ in $G\alpha_{i3}$ knockouts and *vice versa*.

## Enhanced expression levels of remaining $G\alpha_i$ isoform

If the generally accepted assumption holds true that $G\alpha_{i2}$ and $G\alpha_{i3}$ proteins are functionally redundant in the heart, we could expect a compensatory upregulation of the remaining $G\alpha_i$ subunit after knockout of the other. We first determined mRNA expression levels for $G\alpha_{i1}$, $G\alpha_{i2}$, $G\alpha_{i3}$, and $G\alpha_o$ in samples from WT, $G\alpha_{i2}^{-/-}$, and $G\alpha_{i3}^{-/-}$ mice using real-time PCR. In ventricular tissue from WT mice, transcripts for all $G\alpha_i$ protein isoforms and $G\alpha_o$ were found in different amounts (Fig. 3A). While $G\alpha_{i2}$ and $G\alpha_{i3}$ are known to be expressed in cardiomyocytes - with $G\alpha_{i3}$ mRNA being clearly less abundant -, $G\alpha_{i1}$ and $G\alpha_o$ are likely transcribed in non-cardiomyocyte ventricular cells [21]. Deletion of $G\alpha_{i2}$ enhanced the mRNA level of $G\alpha_{i3}$ (to $187\pm21\%$, n = 3, $p<0.05$ vs. WT), as expected [6,22]. In cardiac tissue of $G\alpha_{i3}^{-/-}$ mice $G\alpha_{i2}$ mRNA levels were upregulated to only $127\pm5\%$ (n = 4, $p<0.05$ vs. WT). No significant changes in $G\alpha_o$ or $G\alpha_{i1}$ mRNA expression levels were detected, which is in line with the assumption, that these G proteins are not expressed in cardiomyocytes (see above and Fig. 3B).

Next, protein expression of $G\alpha_i$ isoforms was analyzed in cell membrane preparations from WT, $G\alpha_{i2}^{-/-}$, and $G\alpha_{i3}^{-/-}$ ventricles by probing with $G\alpha_{common}$ antibodies subsequent to high resolution urea/SDS-PAGE-separation of proteins. WT mice expressed both $G\alpha_{i2}$ and $G\alpha_{i3}$ subunits with the protein level of $G\alpha_{i2}$ being much higher than that of $G\alpha_{i3}$ (Fig. 3C), in line with previous studies (e.g. [22]). As expected, in hearts from $G\alpha_{i2}^{-/-}$ mice $G\alpha_{i3}$ was found and $G\alpha_{i2}$ was absent while in hearts from $G\alpha_{i3}^{-/-}$ mice, only $G\alpha_{i2}$ was detectable (Fig. 3C). The specificity of the detected $G\alpha_{i2}$ and $G\alpha_{i3}$ protein bands in $G\alpha_{i2}^{-/-}$, $G\alpha_{i3}^{-/-}$ and WT cardiac tissue was confirmed by analyzing the expression of $G\alpha_i$ isoforms by PTX-mediated [$^{32}$P]ADP ribosylation [23] (data not shown). These experiments prove that gene deletion indeed led to loss of the $G\alpha$ subunit. Statistical analysis of relative expression levels obtained from immunoblots (Fig. 3D) show that $G\alpha_{i2}$ protein is significantly upregulated in ventricles obtained from $G\alpha_{i3}^{-/-}$ mice (to $131\pm10\%$, n = 8, $p<0.05$ vs. WT). However, $G\alpha_{i3}$ protein is much more markedly upregulated upon $G\alpha_{i2}$ deficiency (to $567\pm59\%$, n = 8, $p<0.05$ vs. WT). Taken together, knockout models examined in this study feature a protein upregulation of the respective other $G\alpha_i$ isoform. These data, together with quantitative mRNA data reported above, suggest that increased levels of $G\alpha_{i2}$ or $G\alpha_{i3}$ may partially compensate for the loss of the deleted other $G\alpha_i$ isoform. Hence, any effect seen so far could be caused by the loss of one $G\alpha_i$ protein and/or compensatory signalling exerted by the other. Unfortunately, double-deficient ($G\alpha_{i2}^{-/-}/G\alpha_{i3}^{-/-}$) mice are not viable [22] and hence cannot be used to directly address this question. However, all $G_i$ proteins can acutely be inactivated by PTX treatment.

## Acute $G_i$ inactivation induces L-VDCC kinetic alterations in $G\alpha_{i3}^{-/-}$ cardiomyocytes

We performed experiments with PTX for acute inactivation of $G_{i/o}$ proteins in cardiomyocytes of WT and $G\alpha_i$-deficient mice. Freshly isolated cardiomyocytes were incubated at 37°C with or without PTX for 3 hours and afterwards maintained and examined at room temperature. It has been shown that this protocol completely ablates $G_i$-mediated signalling, e.g. when triggered by adenosine receptors [24]. Of note, the 3 hours incubation phase – even in the absence of PTX – reduced current density in $G\alpha_{i3}$-deficient cells (Fig. 4A). Notably, similar to WT cells, PTX treatment in $G\alpha_{i3}^{-/-}$ myocytes induced a shift of $V_{0.5}$ for steady state inactivation to more negative potentials (to $-22.7\pm1.1$ mV, n = 11; Fig. 4B). Likewise, the recovery from inactivation in $G\alpha_{i3}^{-/-}$ cardiomyocytes was slowed by PTX treatment (to $\tau$: $350\pm27$ ms, n = 8 $p<0.05$ vs. WT; Fig. 4C). In contrast, the calcium current phenotype in $G\alpha_{i2}^{-/-}$ cells was preserved with time and resistant to treatment with PTX. To

**Table 1.** Steady-state inactivation parameters.

| Parameter | WT | $G\alpha_{i2}^{-/-}$ | $G\alpha_{i3}^{-/-}$ |
|---|---|---|---|
| $V_{0.5}$ (mV) | $-19.1\pm0.7$ | $-23.4\pm1.0$*† | $-18.2\pm0.9$ |
| Slope factor (mV) | $5.2\pm0.2$ | $8.7\pm0.6$*† | $5.4\pm0.2$ |

In $G\alpha_{i2}^{-/-}$ cardiomyocytes $V_{0.5}$ of the steady-state inactivation is significantly shifted to more negative potentials. In addition, Boltzmann fits revealed a significant flattening of the curves as indicated by increased slope factors.
*$p<0.05$ vs. WT,
†$p<0.05$ vs. $G\alpha_{i3}^{-/-}$.
doi:10.1371/journal.pone.0024979.t001

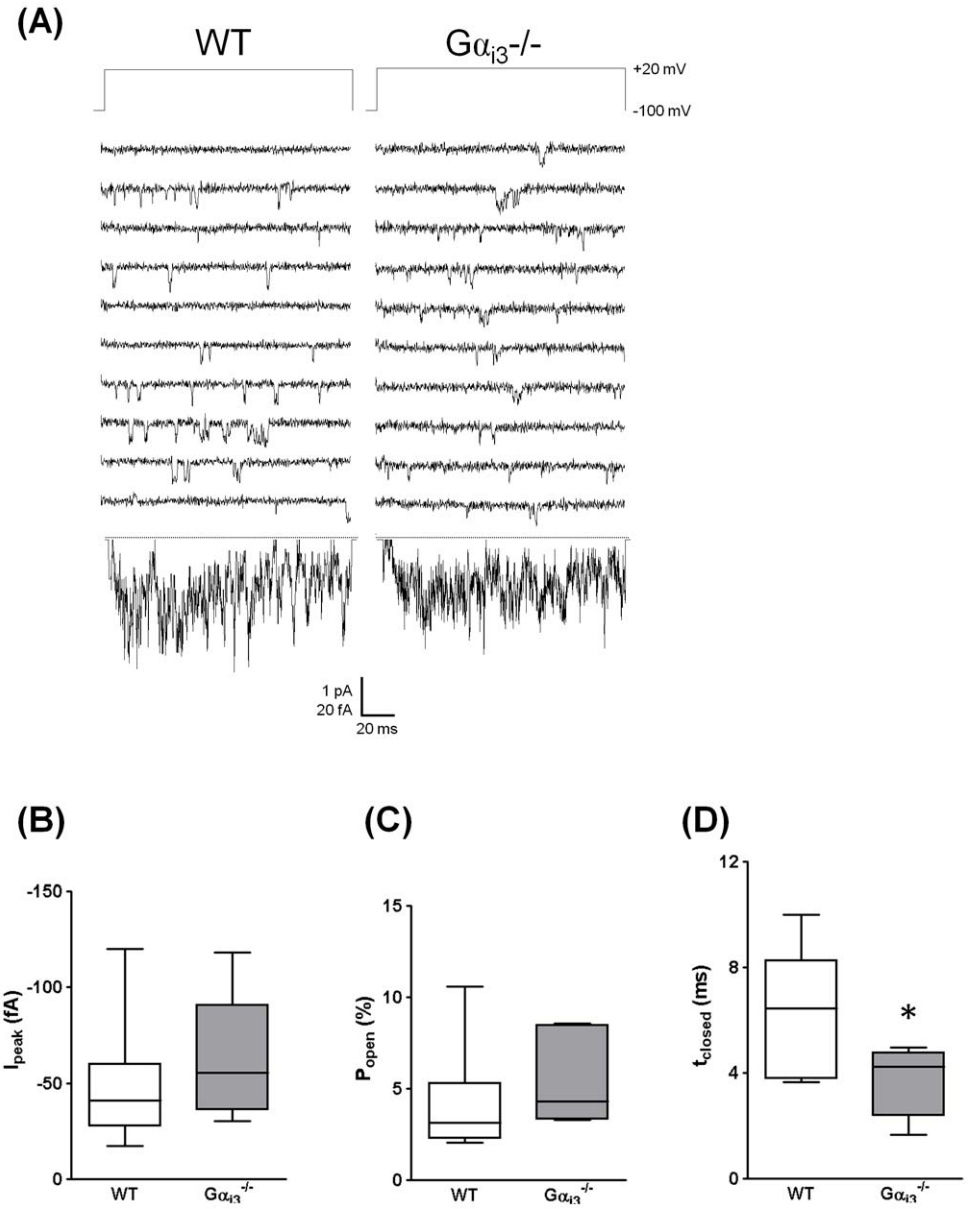


**Figure 2. Single-channel properties of L-type calcium channels.** (A) Exemplary traces of barium currents show increased single-channel activity in ventricular myocytes of $G\alpha_{i3}^{-/-}$ animals vs. WT mice. (B) The peak ensemble average current is $-61\pm13$ fA in $G\alpha_{i3}^{-/-}$ (n = 6) and $-44\pm9$ fA in WT mice (n = 7). (C) The open probability within active sweeps is slightly enhanced in $G\alpha_{i3}^{-/-}$ (5.4±1.0% vs. 4.0±0.9% WT) whereas (D) the mean closed time is significantly reduced ($G\alpha_{i3}^{-/-}$ 3.8±0.5 ms vs. 6.6±0.9 ms WT). Unitary amplitude was not different with $-0.83\pm0.02$ pA (WT) and $-0.79\pm0.03$ pA ($G\alpha_{i3}^{-/-}$). *$p<0.05$ vs. WT. Box-and-whisker plots indicate minimum and maximum values as well as 25th, 50th and 75th percentiles.
doi:10.1371/journal.pone.0024979.g002

summarize, PTX alters channel regulation in cells from $G\alpha_{i3}^{-/-}$ but not from $G\alpha_{i2}^{-/-}$ mice. In $G\alpha_{i3}^{-/-}$, acute PTX treatment – and thus inactivation of $G\alpha_{i2}^{-/-}$ – mimics the kinetic changes induced by chronic gene deletion of $G\alpha_{i2}^{-/-}$. In contrast, the effect of $G\alpha_{i3}$ gene deletion appears to be transient and does not interfere with channel kinetics. Because some of the calcium current changes reported here may be caused by (long-term) structural alterations rather than (acute) functional modulation of calcium channels, we next examined channel composition.

## No significant structural modification of L-VDCC

To obtain insight into the effects of specific and constitutive $G\alpha_i$-deficiency on L-VDCC structure and expression, we determined RNA expression levels of the pore forming $Ca_v\alpha_1$ subunit and the predominant murine cardiac $Ca_v\beta$ subunit, $Ca_v\beta_2$ [14,16,25], which is involved in calcium channel trafficking and gating [26,27,28]. The $Ca_v\beta_2$ subunit mRNA expression in ventricles from $G\alpha_{i2}^{-/-}$ and $G\alpha_{i3}^{-/-}$ animals is not altered compared to WT expression profile (Fig. 5B). In $G\alpha_{i2}^{-/-}$ and $G\alpha_{i3}^{-/-}$ ventricles, the pore forming $Ca_v\alpha_1$ subunit mRNA (Fig. 5B) and membrane protein (Fig. 5C and D) expression levels exhibit only slight and insignificant changes. Thus, these data do not suffice to explain the $G\alpha_i$ isoform-specific regulation of the current density. Therefore, we next switched to the posttranslational level and addressed signalling pathways that are involved in $G_i$ protein-mediated action.

**Table 2.** Single-channel gating in WT and $G\alpha_{i3}^{-/-}$ myocytes.

| Parameter | WT | $G\alpha_{i3}^{-/-}$ |
|---|---|---|
| **i [pA]** | −0.81±0.02 | −0.80±0.03 |
| **$I_{peak}$ [fA]** | −48±13 | −61±12 |
| **$f_{active}$ (%)** | 76±4 | 83±7 |
| **$P_{open}$ (%)** | 4.2±1.1 | 5.4±1.0 |
| **$t_{open}$ [ms]** | 0.48±0.06 | 0.29±0.02* |
| **$\tau_{open}$ [ms]** | 0.42±0.05 | 0.26±0.03* |
| **$t_{closed}$ [ms]** | 6.5±0.9 | 3.8±0.5* |
| **$\tau_{closed,1}$ [ms]** | 0.34±0.02 | 0.36±0.04 |
| **$\tau_{closed,2}$ [ms]** | 15.5±1.5 | 10.2±1.7* |
| **proportion ($\tau_{closed,1}$:$\tau_{closed,2}$)** | 2.0±0.4 | 2.2±0.3 |
| **fl [ms]** | 27.1±4.1 | 18.6±2.4 |

Analysis of single-channel gating parameters in ventricular myocytes from WT (n = 7) and $G\alpha_{i3}^{-/-}$ (n = 6) mice. Recordings with more than one channel were excluded from the analysis. i: unitary current; $I_{peak}$: peak ensemble average current; $f_{active}$: fraction of traces showing at least one opening; $P_{open}$: open probability in active traces; $t_{open}$: mean duration of openings; $\tau_{open}$: dwell time constant of the open state; $t_{closed}$: mean duration between two consecutive openings; $\tau_{closed,1}$: dwell time constant of the fast closed time component; $\tau_{closed,2}$: dwell time constant of the slow closed time component; proportion: ratio of events conferring to either the fast or the slow closed time component; fl: mean latency until the first opening.
*: $p<0.05$ vs. WT.
doi:10.1371/journal.pone.0024979.t002

## Akt activation is unaltered by deletion of $G\alpha_{i2}$ or $G\alpha_{i3}$

Cardiac $G\alpha_i$ is known to activate the PI3-kinase Akt/PKB pathway [29], and Akt-mediated β-subunit phosphorylation prevents $Ca_v\alpha_1$ degradation [30]. A $G_i$-isoform-specific regulation of Akt could explain the calcium current increase in the case of $G\alpha_{i3}^{-/-}$ and decrease in case of $G\alpha_{i2}^{-/-}$. To examine the functional significance of $G\alpha_i$-dependent activation of Akt *in vivo*, animals were treated with either saline or the muscarinic receptor agonist carbachol (CCh, 0.5 mg/kg body weight) by i.p. injection; 15 min later animals were killed, and signalling activity was assessed in heart preparations. Phosphorylation of Akt and its downstream effector glycogen synthase kinase-3α/β (GSK3α/β), were increased in cardiac tissue from all mouse strains after treatment with CCh (Fig. 6A). Although the basal phosphorylation of Akt in $G\alpha_{i2}^{-/-}$ and $G\alpha_{i3}^{-/-}$ cardiac tissue was slightly increased compared to WT (to 138±44% and 143±58% of WT, respectively), we could not observe statistically significant differences between CCh stimulated WT (233±14% to basal), $G\alpha_{i2}^{-/-}$ (201±27%) and $G\alpha_{i3}^{-/-}$ (195±25%) mice (each n = 3). Importantly, the total amount of Akt was not changed in all mice models. Thus, $G_i$-subtype specific channel regulation seems to be independent of Akt phosphorylation in the investigated knockout models.

## Lack of $G\alpha_{i2}$ protein abolishes ERK1/2 activation

Recently, a marked increase of L-type calcium channel density that involved PKC-dependent activation of the ERK1/2 pathway was reported [31]. To determine its involvement, we measured the

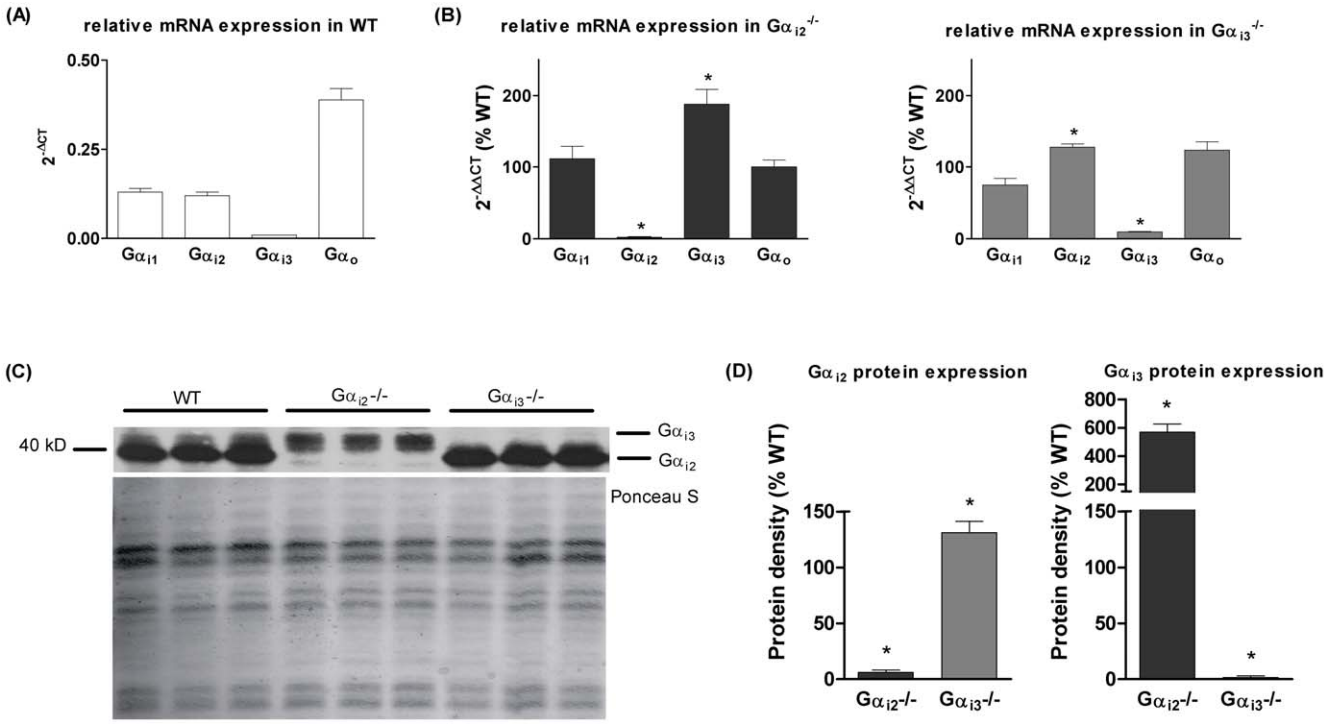


**Figure 3. RNA expression levels of cardiac $G\alpha_{i/o}$ isoforms measured by real-time PCR.** GAPDH was used as endogenous control, and WT mice as calibrator (expression = 100%; n = 4). (A) $2^{-\Delta CT}$ values were calculated to analyze the relative expression of $G\alpha_{i/o}$ isoforms in WT cardiomyocytes. (B) The relative mean expression ($2^{-\Delta\Delta CT}$) reveals a significantly increased $G\alpha_{i3}$ mRNA content in ventricular tissue of $G\alpha_{i2}^{-/-}$ mice (n = 3) and significantly increased $G\alpha_{i2}$ mRNA levels in $G\alpha_{i3}^{-/-}$ mice (n = 4). (C) Representative example of $G\alpha_{i2}$ and $G\alpha_{i3}$ protein expression in murine ventricular tissue from WT, $G\alpha_{i2}^{-/-}$ and $G\alpha_{i3}^{-/-}$ mice. Cell membranes were isolated and $G\alpha_i$ proteins were analyzed by immunoblotting using an anti-$G\alpha_{common}$ antibody. Shorter exposure times were used to analyse $G\alpha_{i2}$ protein. (D) Summarized protein expression data show an upregulation of $G\alpha_{i3}$ in $G\alpha_{i2}^{-/-}$ mice and an upregulation of $G\alpha_{i2}$ in $G\alpha_{i3}^{-/-}$ mice (n = 8). *$p<0.05$ vs. WT.
doi:10.1371/journal.pone.0024979.g003

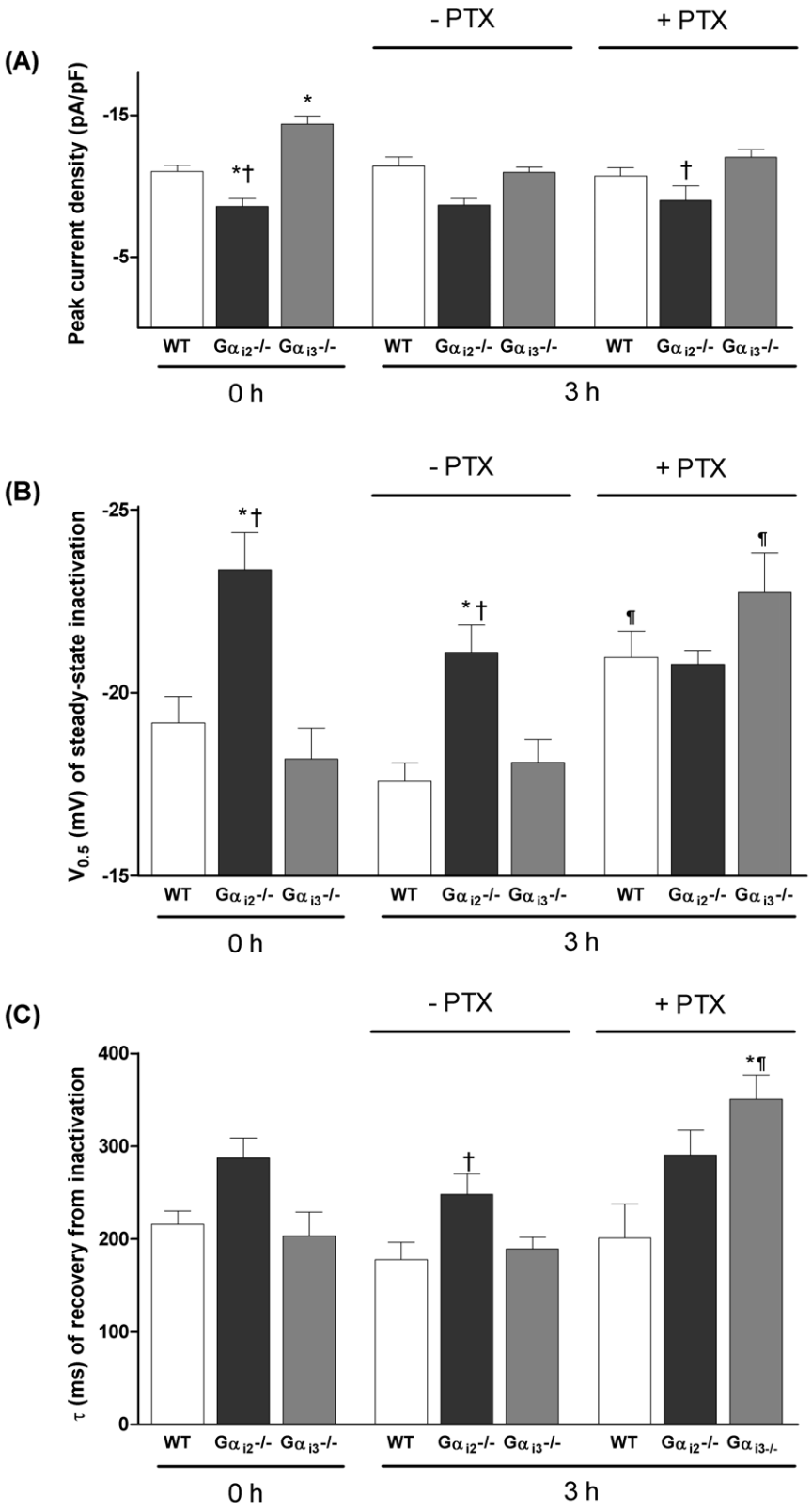


**Figure 4. Effects of acute inactivation of $G_{i/o}$ proteins by PTX incubation of isolated cardiac myocytes.** (A) Effects of PTX on peak L-VDCC current density. PTX treatment by itself did not affect calcium current density. (B) Effects of PTX on steady-state inactivation, as gauged by the midpoint voltage $V_{0.5}$ of a Boltzmann function. No change is seen after 3 hours of drug-free incubation compared to 0 hour. PTX leads to a significant leftward shift of $V_{0.5}$ in WT (from $-19.2\pm0.7$ mV to $-21.0\pm0.7$ mV, n = 7–18) and $G\alpha_{i3}^{-/-}$ (from $-18.2\pm0.7$ mV to $-22.7\pm1.1$ mV, n = 11–13). (C) PTX affects the recovery of the L-VDCC from inactivation. PTX inhibits the channel recovery in $G\alpha_{i3}^{-/-}$ ($\tau$ from $189\pm12$ ms to $350\pm26$ ms, n = 5–11). *$p<0.05$ vs. WT, †$p<0.05$ vs. $G\alpha_{i3}^{-/-}$, ¶$p<0.05$ vs. 3 h without PTX.
doi:10.1371/journal.pone.0024979.g004

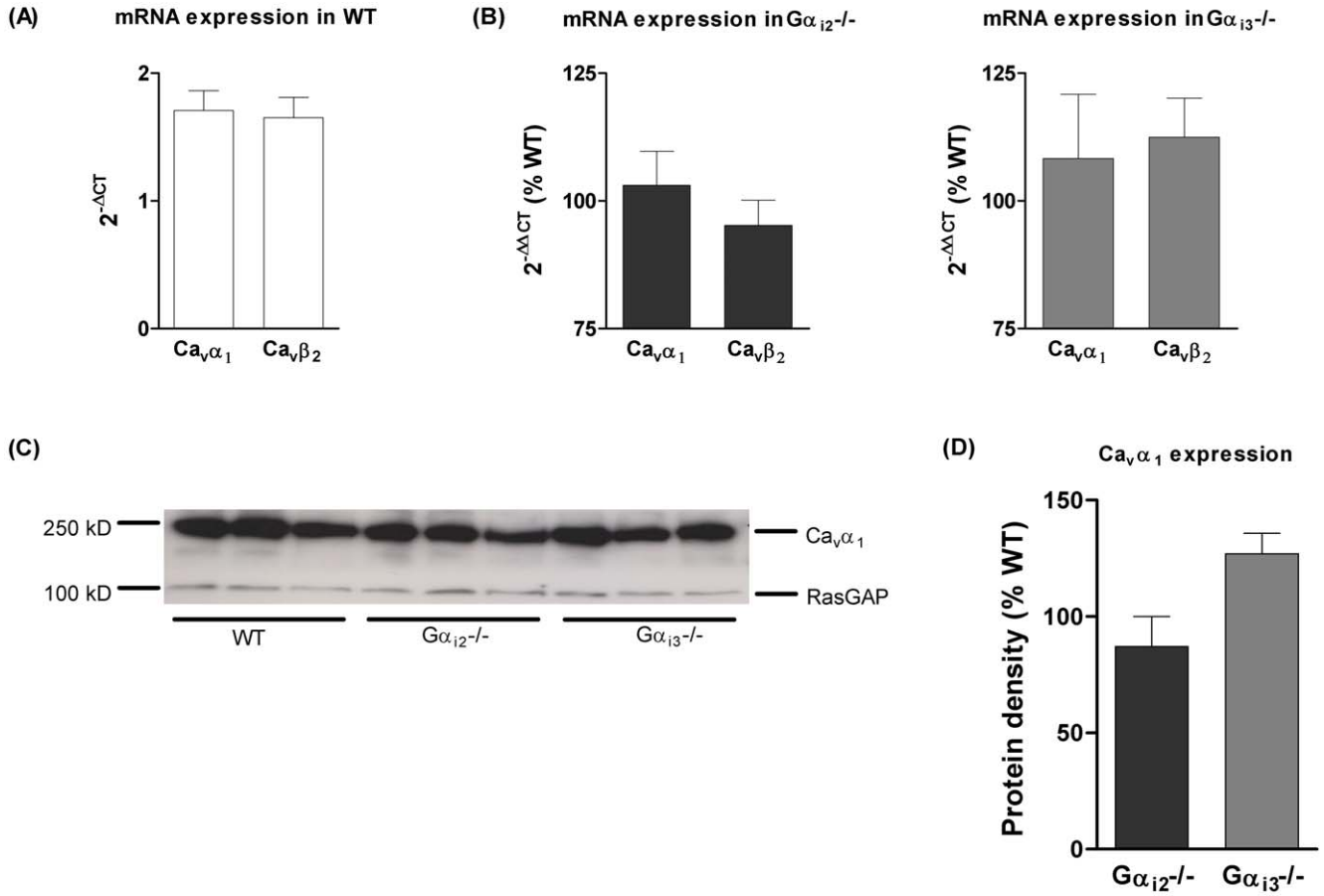


**Figure 5. Calcium channel subunit expression.** (A) $2^{-\Delta CT}$ values were calculated against GAPDH expression to analyze the relation of L-type calcium channel subunits in WT cardiomyocytes (n = 4). (B) No significant changes in the relative mean expression ($2^{-\Delta\Delta CT}$) were observed in ventricular tissues from $G\alpha_{i2}^{-/-}$ (n = 3) and $G\alpha_{i3}^{-/-}$ mice (n = 4). (C) Representative example of $Ca_v\alpha_1$ protein expression in murine ventricular tissue from WT, $G\alpha_{i2}^{-/-}$ and $G\alpha_{i3}^{-/-}$ mice. (D) Quantification of $Ca_v\alpha_1$ protein levels show no change in ventricles from $G\alpha_{i3}^{-/-}$, $G\alpha_{i2}^{-/-}$ and WT mice (n = 3).
doi:10.1371/journal.pone.0024979.g005

activation of ERK1/2 protein in total cardiac tissue. $G\alpha_{i2}^{-/-}$ mice demonstrated a significantly blunted increase of ERK1/2 phosphorylation in CCh-stimulated animals (128±5% to basal, n = 3) compared to WT (268±6%, n = 3) and $G\alpha_{i3}^{-/-}$ (192±20%, n = 3) cardiomyocytes. Of note, in $G\alpha_{i2}^{-/-}$ and $G\alpha_{i3}^{-/-}$ cardiac tissues, the basal ERK1/2 phosphorylation levels were increased compared to WT basal phosphorylation (Fig. 6B), while the total amount of ERK1/2 in the heart was the same in all mouse models tested. These results indicate a $G\alpha_{i2}$-dependent ERK1/2 phosphorylation and strongly suggest that ERK1/2 plays an important role in isoform-specific $G\alpha_i$ protein signalling.

## Discussion

The two inhibitory G protein isoforms $G_{i2}$ and $G_{i3}$ are both upregulated in heart failure [6,7,8]. One functionally important target of $G_i$ protein signalling is the L-VDCC, the crucial trigger of cardiac excitation-contraction coupling. $G_i$-protein-mediated inhibition of L-VDCC has been demonstrated for $\beta_2$-adrenergic [4] and muscarinic [20] receptor signalling. In this context, we previously provided single-channel evidence that $G\alpha_{i2}$ does not confer the L-VDCC inhibition observed in mice with chronic overexpression of the $\beta_2$-adrenergic receptor [18]. On the other hand, cardiac $G\alpha_{i2}$ (but not $G\alpha_{i3}$) seems necessary and sufficient to mediate the muscarinic receptor-mediated L-VDCC inhibition [20], presumably through the classical adenylyl cyclase pathway. So far, no isoform-specific function could be assigned to cardiac $G\alpha_{i3}$; however, $G_{i3}$ has been shown to be an exclusive and specific regulator of autophagy in the liver [22,32].

The different behaviour of L-VDCC currents obtained with isolated myocytes from $G\alpha_{i2}^{-/-}$ and $G\alpha_{i3}^{-/-}$ mice shown here and previously [18] demonstrates contrasting functional roles of these two $G\alpha_i$ isoforms. Although the issue has also been addressed by others [19,20,33], our study is the first to demonstrate small but significant changes of basal whole-cell current density: a reduction in myocytes from $G\alpha_{i2}^{-/-}$ mice and an increase in myocytes from $G\alpha_{i3}^{-/-}$ mice. The altered steady-state inactivation and recovery observed with $G\alpha_{i2}^{-/-}$ under basal conditions (Fig. 1C and D), and with $G\alpha_{i3}^{-/-}$ myocytes after PTX treatment (Fig. 4B and C), point to a modulation of gating properties specific to $G\alpha_{i2}$. In contrast to data presented here, Nagata *et al.* [20] did not detect a significant difference in L-VDCC activity between myocytes from WT, $G\alpha_{i2}^{-/-}$ and $G\alpha_{i3}^{-/-}$ mice. With respect to $G\alpha_{i2}^{-/-}$, this finding can be explained by the different prepulse potentials: the prepulse voltages (−50 mV used by Nagata and co-workers vs. −40 mV in our case) - intended to inactivate primarily sodium currents - lie within the descending part of steady-state inactivation (Fig. 1C). This likely translates into the more reduced peak in the

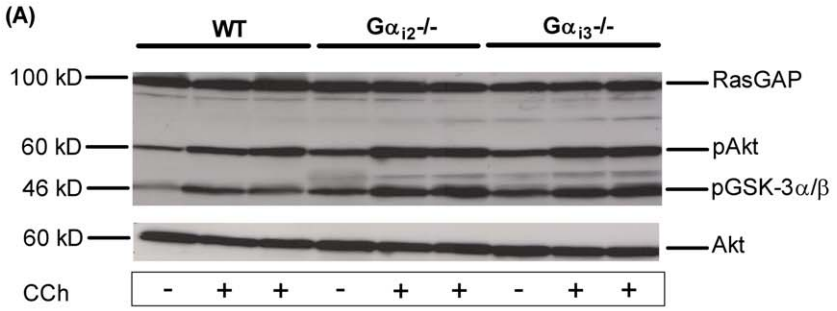
(A)
WT
Gαi2-/-
Gαi3-/-
100 kD
RasGAP
60 kD
pAkt
46 kD
pGSK-3α/β
60 kD
Akt
CCh
- + + - + + - + +

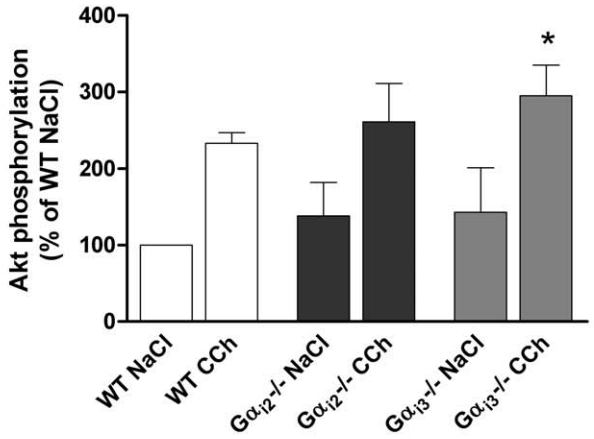
Akt phosphorylation (% of WT NaCl)
400
300
200
100
0
*
WT NaCl
WT CCh
Gαi2-/- NaCl
Gαi2-/- CCh
Gαi3-/- NaCl
Gαi3-/- CCh

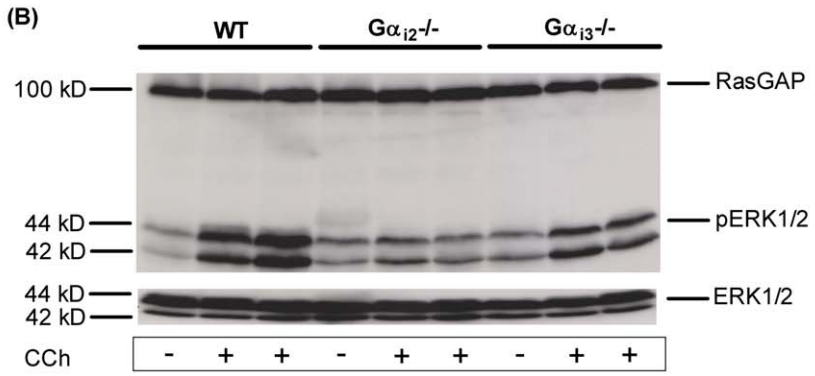
(B)
WT
Gαi2-/-
Gαi3-/-
100 kD
RasGAP
44 kD
42 kD
pERK1/2
44 kD
42 kD
ERK1/2
CCh
- + + - + + - + +

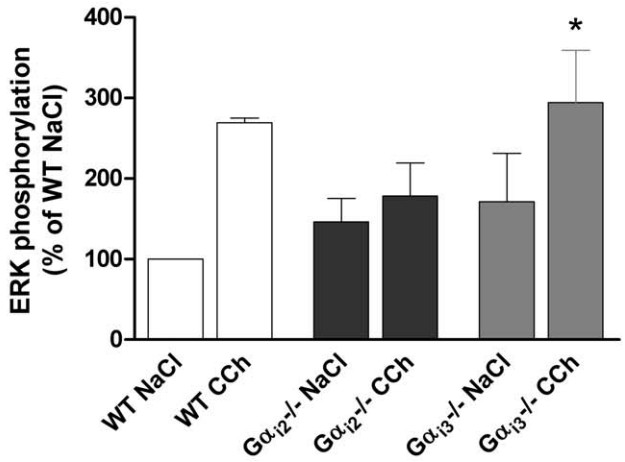
ERK phosphorylation (% of WT NaCl)
400
300
200
100
0
*
WT NaCl
WT CCh
Gαi2-/- NaCl
Gαi2-/- CCh
Gαi3-/- NaCl
Gαi3-/- CCh

**Figure 6. Signalling events downstream of $G\alpha_i$ stimulation.** Representative western blot of cardiac tissues of animals treated either with saline or CCh (0.5 mg/kg body weight) for 15 min. (A) Western Blot and densitometry analyses of ventricular homogenates show that Akt phosphorylation was significantly and to a similar extent increased after CCh stimulation in all genotypes (n = 3). Total amount of Akt protein was unaltered and was used as loading control. (B) Western blot showing ERK1/2 phosphorylation and total ERK1/2 expression and bar graphs of combined results expressed as increase in pERK1/2 normalized to total ERK1/2 and compared to saline treated WT mice. The increase of ERK1/2 activation in CCh treated cells was markedly inhibited by $G\alpha_{i2}$ gene deletion compared to WT and $G\alpha_{i3}^{-/-}$ mice (n = 3). *$p<0.05$ vs. WT NaCl.
doi:10.1371/journal.pone.0024979.g006

current voltage plot in our study. Interestingly, Zuberi *et al.* [19] compared $G\alpha_{i2}^{-/-}$ mice with $G\alpha_{i1}^{-/-}/G\alpha_{i3}^{-/-}$ double knockout mice and found distinct effects on surface ECGs: in $G\alpha_{i2}^{-/-}$ animals (but not in the double knockout mice), the effective refractory period was reduced and ventricular arrhythmias were induced more easily. In summary, $G\alpha_{i2}$ protein deletion showed dramatic consequences on channel regulation *in vivo* and *ex vivo*.

There are no changes of cardiac L-VDCC composition regarding the main cardiac L-VDCC subunits, $Ca_v\alpha_1$ and $Ca_v\beta_2$ (Fig. 5B and D) that would explain the obtained effects on current density. Furthermore, because of the compensatory upregulation of the remaining $G\alpha_i$ isoform in case of either $G\alpha_{i2}$ or $G\alpha_{i3}$ deficiency (Fig. 3B and D), it is difficult to attribute the observed changes in L-VDCC regulation/function to the higher expression of one $G\alpha_i$ isoform or to the loss of the other or to both. Therefore, given the novel functional effects reported here for cardiac $G\alpha_{i2}$ and $G\alpha_{i3}$, we have to consider a number of molecular pathways. For instance, activation of Stim1 [34] may lead to altered L-VDCC function and subcellular distribution. Enhanced endocytosis and degradation of calcium channels can also be mediated by activation of PIKfyve [35] and subsequent $Ca_v\alpha_1$ targeting to lysosomes. Further, the RGK proteins Rad and Rem expressed in the heart [36] are appealing candidates, because they negatively regulate both membrane expression and gating of L-VDCC [37,38] while little is known about how these small GTP-binding proteins are regulated themselves [39]. In our present study, we focused on two other important molecular pathways since they are significantly regulated by $G_i$-signalling. First, PI3-kinase Akt/PKB signalling is known to be activated by cardiac $G\alpha_i$ [29], and Catalucci *et al.* [30] revealed a mechanism through which the PI3-kinase Akt/PKB pathway modulates $Ca^{2+}$ entry in cardiac cells via L-VDCC. Our data showed a CCh-induced Akt phosphorylation independent of the deletion of either $G\alpha_i$ isoform (Fig. 6A). Second, it was demonstrated that deactivation of $G_i$ leads to a significant reduction in ERK1/2 phosphorylation and that this effect was $G_s$- and $G_q$- independent [29,40]. In the present study, we have shown that $G\alpha_{i2}$ deletion prevents phosphorylation of ERK1/2. Recently, Smani *et al.* [31] found a leftward shift and a marked increase in L-VDCC density induced by urocortin, which involved PKC-dependent activation of the MAPK-ERK1/2 pathway. Based on these findings we propose that loss of activation of L-VDCC by ERK1/2 might be a mechanism involved in functional regulation of calcium current in $G\alpha_{i2}$ deficient mice.

A change of $G\alpha_s$ mediated signalling might account for altered calcium currents when a $G\alpha_i$ is lacking. With this caveat in mind, we demonstrated in our previous study that $G\alpha_s$ protein expression remained unaffected in hearts from mice deficient in the major isoform $G\alpha_{i2}$ [18]. Yet, possible changes in associated proteins like $G\beta\gamma$ subunits might indirectly affect $G\alpha$ mediated signalling [41]. Indeed, we observed that expression of $G\beta_{1/2}$ was slightly reduced in $G\alpha_{i2}^{-/-}$, but not $G\alpha_{i3}^{-/-}$ (data not shown). In any case, our single-channel analysis (in particular, the decrease in open time) does not support the idea of enhanced $G\alpha_s$ mediated, cAMP-mediated signalling in $G\alpha_{i3}$-deficient hearts (Table 2).

The data presented here could not elucidate all effects seen in the knockout animals. Thus, eventually, $G_{i3}$'s role in L-VDCC regulation remains unclear, mainly in light of the absence of acute PTX effects in $G\alpha_{i2}^{-/-}$ mice. However, due to the effects seen by incubation without PTX, our findings suggest that the increment in channel activity observed in the absence of $G\alpha_{i3}$ might be driven by an *in vivo* mechanism, which is not preserved *ex vivo* (Fig. 4A). It has also to be pointed out that the immunoblot data reveal total cardiac membrane channel protein levels, which does not necessarily match up the fraction of functional channels located in the sacrolemma. Given our currently available methods to analyze the subcellular localization of calcium channels and their regulation, all of these ideas require further work, which for technical reasons has to be done in recombinant systems.

Taken together, our data reported here and in a previous paper [18] point to the (patho-) physiological importance of subtype-specific $G_i$ protein signalling in the heart. In particular, in terminal heart failure, $G\alpha_{i2}$ upregulation now appears as an attractive mechanism linked to remodelling of L-VDCC [13,14,15,16]. Therefore, the present study provides new insights into potential mechanisms linking modulation of L-VDCC to the inhibitory G protein isoform $G_{i2}$ in cardiomyocytes, and highlights $G_{i2}$-specific signalling via ERK1/2. Further research needs to focus on detailed signalling pathways involving ERK1/2.

## Methods

### Ethic statement

Animal breeding, maintenance and experiments were approved by the responsible federal state authority (Landesamt für Natur-, Umwelt- und Verbraucherschutz Nordrhein-Westfalen; reference No. K 27, 24/04 and 8.87-51.05.20.09.232) and the responsible local authority (Umwelt- und Verbraucherschutzamt der Stadt Köln; reference No. 576/1.36.6.3.-47/08 Be). All animal experiments conform with the *Guide for the Care and Use of Laboratory Animals* published by the US National Institutes of Health (NIH Publication No. 85-23, revised 1996).

### Animals

Generation, breeding and characterization of $G\alpha_{i2}$- or $G\alpha_{i3}$-deficient mice have been described previously [18,22,42,43,44,45]. All $G\alpha_i$-deficient mouse strains used were backcrossed onto a C57Bl6 background for >10 generations. Knockout and WT control mice were maintained at the animal facilities of the Heinrich-Heine-University, Düsseldorf, and of the Department of Pharmacology at the University of Cologne. Mice analyzed in this study were of both sexes, 3–9 months of age and weighted 20–35 g.

### Genotyping

Tail-clip analysis was performed on 3–4 weeks old mice. Genomic DNA was prepared and genotyping PCR for $G\alpha_{i2}$ and $G\alpha_{i3}$ was performed as described previously [18,43].

### Real time PCR

Primer for $G\alpha_{i1}$, $G\alpha_{i2}$, $G\alpha_{i3}$ isoforms and $Ca_v\alpha_1$ subunit were described previously [25,46]. Specific primers for the $G\alpha_o$ and $Ca_v\beta_2$ subunit were designed using Primer Express Software v3.0

(Applied Biosystems, Foster City, USA). For $G\alpha_o$: 5′-TGGC-ATCGTAGAAACCCACTT-3′ (sense) and 5′-CGACGTCAAA-CAGCCTGAAG-3′ (antisense) and for $Ca_v\beta_2$: 5′-GGGAGG-CAGTACGTAGAGAAGCT-3′ (sense) and 5′-TGCAAATG-CAACAGGTTTT GTC-3′ (antisense). Total cellular RNA was extracted from murine heart (ventricle) according to the manufacturer's protocol (Qiagen QIAshredder and RNeasy Mini Kit, Qiagen, Hilden, Germany). For qualitative analysis of RNA integrity, 2 µg of total RNA was separated on a 1% formaldehyde agarose gel. Total RNA was subsequently converted into cDNA by ImProm-II Reverse Transcription Kit (Promega, Mannheim, Germany). Real-time PCR was carried out using the 7500 Real-Time PCR system (Applied Biosystems) under standard conditions with 200 pM PCR primers. Each sample was analyzed in triplets using SYBR green (Applied Biosystems) as fluorescent detector and GAPDH as endogenous control.

## Cell membrane preparation

Murine cardiac ventricles were disrupted and homogenised in a lysis buffer containing 10 mM Tris-HCl (pH 7.4), 1 mM EDTA, 0.5 mM DTT, and an EDTA-free protease inhibitor cocktail (Roche, Penzberg, Germany) using an ultra-turrax blender. Cellular membranes were isolated by two steps of centrifugation at 450 g and 30.000 g. Membrane pellets were subsequently dissolved in a buffer consisting of a freezing supplement (70 mM Tris (pH 7.4), 12 mM $MgCl_2$, 60% Glycerol, 240 µg/µl DNAse) and the lysis buffer in a ratio of 1:6 in order to stabilize membrane-associated proteins.

## Phosphorylation assay

Animals were injected i.p. with 0.5 mg/kg carbachol (CCh) diluted in 0.9% normal saline. Sham injections were performed with 400 µl 0.9% saline per 30 g weight. After 15 min ventricular tissue was harvested and lysed in buffer (50 mM HEPES, 1% Triton, 50 mM NaCl, 10 mM $Na_3VO_4$, 0.1% SDS, 0.1 M NaF, 10 mM EDTA, complete mini protease inhibitor, pH 7.4) and left for 30 min at 4°C. Total cell lysates were extracted from the supernatant by centrifugation at 13.500 g for 20 min.

## Immunoblotting

$G\alpha_i$ and $Ca_v\alpha_1$ proteins isolated from cell membranes were separated on 6 M urea/9% SDS-PAGE gels (protein content per lane was 90 µg) and on 8% SDS-PAGE gels (protein content per lane was 100 µg), respectively [22]. Protein kinase B/Akt and ERK1/2 in total cell lysates were separated on 10% SDS-PAGE gels (100 µg protein content per lane). Separated proteins were blotted onto nitrocellulose membranes (Hybond C extra; Amersham Bioscience). $G\alpha_i$ proteins were detected with an anti-$G\alpha_{common}$ antibody [45] (1:1000) and $Ca_v\alpha_1$ with an anti-$Ca_v\alpha_1$ antibody (1:200; Sigma Aldrich). For detection of phosphorylation, membranes were incubated with phospho-Akt (Ser473), phospho-GSK3α/β (Ser21/9) and phospho-ERK1/2 (Thr202/Tyr204) antibodies. Membranes were reprobed with Akt and ERK1/2 antibodies (each 1:1000; Cell Signalling) after stripping. Emitted light of stained membranes were captured on films and developed in different expositions. Protein densities were calculated using Aida Image Analyzer (Raytest, Straubenhardt, Germany) software. The Ras-GTP-activating protein (RasGAP; [47]) was used as a loading control for $Ca_v\alpha_1$. Equal loading on blotting membrane for $G\alpha_i$ proteins was controlled by a non-specific protein staining using Ponceau S. Only blots with equal loading were analyzed. To confirm $G\alpha_i$ band specificity, we performed ADP ribosylation of PTX-sensitive G proteins as described [23].

## Cardiomyocyte isolation

Single ventricular myocytes were isolated from hearts of 3–9 months old mice by enzymatic dissociation using a method described previously [48]. Only rod shaped cardiomyocytes were used for the experiments. Cells were maintained at room temperature and subjected to patch-clamp analysis. If indicated, a fraction of isolated ventricular myocytes was incubated without or with 1.5 µg/ml of PTX (Sigma Aldrich, St. Louis, USA) for 3 hours at 37°C [24].

## Single-channel measurements

Single-channel patch clamp recordings were done in the cell-attached configuration as reported [18]. The composition of bath solution was (mM): K-glutamate 120, KCl 25, $MgCl_2$ 2, HEPES 10, EGTA 2, $CaCl_2$ 1, $Na_2$-ATP 1, glucose 10 (pH 7.4 with KOH). Patch pipettes (7–9 MΩ) contained (mM): $BaCl_2$ 70, HEPES 10, sucrose 110 (pH 7.4 with TEA-OH). Barium currents were recorded at room temperature using a holding potential of −100 mV and depolarizing test pulses to +20 mV (duration 150 ms, frequency 1.66 Hz, 180 sweeps per experiment minimum). Data were sampled at 10 kHz and filtered at 2 kHz using an Axopatch 200A amplifier (Axon Instruments, Sunnyvale, CA, U.S.A.). Only experiments with one single active channel in the patch were analyzed (identified by the lack of stacked openings).

## Whole-cell current measurements

Conventional whole-cell patch clamp recordings were performed with cells maintained at room temperature in bath solution containing (mM): NaCl 137, CsCl 5.4, $CaCl_2$ 2, $MgCl_2$ 1, glucose 10, HEPES 10 (pH 7.4 with NaOH). Pipette (2–3 MΩ) solution was composed of (mM): CsCl 120, $MgCl_2$ 1, Mg-ATP 4, EGTA 10, HEPES 5 (pH 7.2 with CsOH). Giga-Ohm seals (resistance 2–5 GΩ) were formed by gentle suction. At the beginning of each experiment, membrane capacitance was measured by means of fast depolarizing ramp pulses from −80 to −85 mV over 25 ms. Cells were depolarized from a holding potential of −80 mV to a 50 ms prepulse to −40 mV in order to inactivate sodium channels. This was followed by test pulse voltages ranging from −40 to +50 mV in 10 mV steps (pulse duration 150 ms). For time-dependent inactivation, the declining raw currents at −10, 0, +10, +20 and +30 mV were fitted by a double-exponential function, yielding fast and slow time constant. For investigation of gating kinetics, standard two-pulse protocols were used: the voltage-dependent inactivation was measured after a prepulse of variable amplitude and 250 ms duration, followed by a test pulse of fixed amplitude for 50 ms. The midpoint voltage $V_{0.5}$ was determined by fitting a Boltzmann function to the data. Recovery from inactivation was determined by two 200 ms depolarizing voltage pulses to 0 mV. The interpulse interval at a holding potential of −45 mV was increased from 50 to 375 ms in 25 ms steps. Recovery was fitted by a mono-exponential function, yielding the recovery time constant τ.

## Statistical analysis

Data are presented as means ± SEM. Patch-clamp data were analyzed using pClamp software (CLAMPEX 6 and FETCHAN, Axon Instruments). Analysis of L-VDCC kinetics was performed as described previously [49] using GraphPad Prism 4. A one-sample t-test was used to analyze normalized data. Differences between genotypes were analyzed by one-way ANOVA followed by Dunnett's or Tukey's post test, and between treatments within one given genotype by two-tailed Student's t tests. For electrophysiological statistics, number of cardiomyocytes from a minimum of 3

animals, and for molecular biology statistics, number of animals was evaluated. P values$<0.05$ were considered statistically significant.

## Acknowledgments

The authors wish to thank Olga Felda and Sigrid Kirchmann-Hecht for excellent technical assistance, Jens Reifenrath for help with animal breeding, and Christian Fabisch, Andreas Markl, Katja Pexa, Markus Schubert and Oliver Stöhr for discussion and support.

## References

1. Hamm HE (1998) The many faces of G protein signaling. J Biol Chem 273: 669–672.
2. Rockman HA, Koch WJ, Lefkowitz RJ (2002) Seven-transmembrane-spanning receptors and heart function. Nature 415: 206–212.
3. Lohse MJ, Engelhardt S, Eschenhagen T (2003) What is the role of β-adrenergic signaling in heart failure? Circ Res 93: 896–906.
4. Xiao RP, Avdonin P, Zhou YY, Cheng H, Akhter SA, et al. (1999) Coupling of $\beta_2$-adrenoceptor to $G_i$ proteins and its physiological relevance in murine cardiac myocytes. Circ Res 84: 43–52.
5. Bohm M, Gierschik P, Knorr A, Larisch K, Weismann K, et al. (1992) Desensitization of adenylate cyclase and increase of $G_i\alpha$ in cardiac hypertrophy due to acquired hypertension. Hypertension 20: 103–112.
6. Eschenhagen T (1993) G proteins and the heart. Cell Biol Int 17: 723–749.
7. Feldman AM, Cates AE, Veazey WB, Hershberger RE, Bristow MR, et al. (1988) Increase of the 40,000-mol wt pertussis toxin substrate (G protein) in the failing human heart. J Clin Invest 82: 189–197.
8. Neumann J, Schmitz W, Scholz H, von Meyerinck L, Doring V, et al. (1988) Increase in myocardial $G_i$-proteins in heart failure. Lancet 2: 936–937.
9. Mittmann C, Pinkepank G, Stamatelopoulou S, Wieland T, Nurnberg B, et al. (2003) Differential coupling of m-cholinoceptors to $G_i/G_o$-proteins in failing human myocardium. J Mol Cell Cardiol 35: 1241–1249.
10. Schroder EA, Wei Y, Satin J (2006) The developing cardiac myocyte: maturation of excitability and excitation-contraction coupling. Ann N Y Acad Sci 1080: 63–75.
11. Abernethy DR, Schwartz JB (1999) Calcium-antagonist drugs. N Engl J Med 341: 1447–1457.
12. Xu X, Colecraft HM (2009) Engineering proteins for custom inhibition of Ca(V) channels. Physiology (Bethesda) 24: 210–218.
13. Gonzalez-Gutierrez G, Miranda-Laferte E, Nothmann D, Schmidt S, Neely A, et al. (2008) The guanylate kinase domain of the β-subunit of voltage-gated calcium channels suffices to modulate gating. Proc Natl Acad Sci U S A 105: 14198–14203.
14. Hullin R, Matthes J, von Vietinghoff S, Bodi I, Rubio M, et al. (2007) Increased expression of the auxiliary $\beta_2$-subunit of ventricular L-type $Ca^{2+}$ channels leads to single-channel activity characteristic of heart failure. PLoS One 2: e292.
15. Jangsangthong W, Kuzmenkina E, Khan IF, Matthes J, Hullin R, et al. (2009) Inactivation of L-type calcium channels is determined by the length of the N terminus of mutant $\beta_1$ subunits. Pflugers Arch 459: 399–411.
16. Link S, Meissner M, Held B, Beck A, Weissgerber P, et al. (2009) Diversity and developmental expression of L-type calcium channel $\beta_2$ proteins and their influence on calcium current in murine heart. J Biol Chem 284: 30129–30137.
17. Wettschureck N, Offermanns S (2005) Mammalian G proteins and their cell type specific functions. Physiol Rev 85: 1159–1204.
18. Foerster K, Groner F, Matthes J, Koch WJ, Birnbaumer L, et al. (2003) Cardioprotection specific for the G protein $G_{i2}$ in chronic adrenergic signaling through $\beta_2$-adrenoceptors. Proc Natl Acad Sci U S A 100: 14475–14480.
19. Zuberi Z, Nobles M, Sebastian S, Dyson A, Lim SY, et al. (2010) Absence of the Inhibitory G-protein, $G\alpha_{i2}$, Predisposes to Ventricular Cardiac Arrhythmia. Circ Arrhythm Electrophysiol;in press; doi:10.1161/CIRCEP.1109.894329.
20. Nagata K, Ye C, Jain M, Milstone DS, Liao R, et al. (2000) $G\alpha_{i2}$ but not $G\alpha_{i3}$ is required for muscarinic inhibition of contractility and calcium currents in adult cardiomyocytes. Circ Res 87: 903–909.
21. Asano T, Kamiya N, Semba R, Kato K (1988) Ontogeny of the GTP-binding protein $G_o$ in rat brain and heart. J Neurochem 51: 1711–1716.
22. Gohla A, Klement K, Piekorz RP, Pexa K, vom Dahl S, et al. (2007) An obligatory requirement for the heterotrimeric G protein Gi3 in the antiautophagic action of insulin in the liver. Proc Natl Acad Sci U S A 104: 3003–3008.
23. Exner T, Jensen ON, Mann M, Kleuss C, Nurnberg B (1999) Posttranslational modification of $G\alpha_{o1}$ generates $G\alpha_{o3}$, an abundant G protein in brain. Proc Natl Acad Sci U S A 96: 1327–1332.
24. Xiao RP, Ji X, Lakatta EG (1995) Functional coupling of the beta 2-adrenoceptor to a pertussis toxin-sensitive G protein in cardiac myocytes. Mol Pharmacol 47: 322–329.
25. Beetz N, Hein L, Meszaros J, Gilsbach R, Barreto F, et al. (2009) Transgenic simulation of human heart failure-like L-type $Ca^{2+}$-channels: implications for fibrosis and heart rate in mice. Cardiovasc Res 84: 396–406.
26. Colecraft HM, Alseikhan B, Takahashi SX, Chaudhuri D, Mittman S, et al. (2002) Novel functional properties of $Ca^{2+}$ channel β subunits revealed by their expression in adult rat heart cells. J Physiol 541: 435–452.
27. Dolphin AC (2003) β subunits of voltage-gated calcium channels. J Bioenerg Biomembr 35: 599–620.
28. Perez-Reyes E, Castellano A, Kim HS, Bertrand P, Baggstrom E, et al. (1992) Cloning and expression of a cardiac/brain β subunit of the L-type calcium channel. J Biol Chem 267: 1792–1797.
29. Chesley A, Lundberg MS, Asai T, Xiao RP, Ohtani S, et al. (2000) The $\beta_2$-adrenergic receptor delivers an antiapoptotic signal to cardiac myocytes through $G_i$-dependent coupling to phosphatidylinositol 3′-kinase. Circ Res 87: 1172–1179.
30. Catalucci D, Zhang DH, DeSantiago J, Aimond F, Barbara G, et al. (2009) Akt regulates L-type $Ca^{2+}$ channel activity by modulating $Ca_v\alpha_1$ protein stability. J Cell Biol 184: 923–933.
31. Smani T, Calderon-Sanchez E, Gomez-Hurtado N, Fernandez-Velasco M, Cachofeiro V, et al. (2010) Mechanisms underlying the activation of L-type calcium channels by urocortin in rat ventricular myocytes. Cardiovasc Res 87: 459–466.
32. Gohla A, Klement K, Nurnberg B (2007) The heterotrimeric G protein G(i3) regulates hepatic autophagy downstream of the insulin receptor. Autophagy 3: 393–395.
33. Chen F, Spicher K, Jiang M, Birnbaumer L, Wetzel GT (2001) Lack of muscarinic regulation of $Ca^{2+}$ channels in $G_{i2}\alpha$ gene knockout mouse hearts. Am J Physiol Heart Circ Physiol 280: H1989–1995.
34. Park CY, Shcheglovitov A, Dolmetsch R (2010) The CRAC channel activator STIM1 binds and inhibits L-type voltage-gated calcium channels. Science 330: 101–105.
35. Tsuruta F, Green EM, Rousset M, Dolmetsch RE (2009) PIKfyve regulates $Ca_v1.2$ degradation and prevents excitotoxic cell death. J Cell Biol 187: 279–294.
36. Finlin BS, Crump SM, Satin J, Andres DA (2003) Regulation of voltage-gated calcium channel activity by the Rem and Rad GTPases. Proc Natl Acad Sci U S A 100: 14469–14474.
37. Yada H, Murata M, Shimoda K, Yuasa S, Kawaguchi H, et al. (2007) Dominant negative suppression of Rad leads to QT prolongation and causes ventricular arrhythmias via modulation of L-type Ca2+ channels in the heart. Circ Res 101: 69–77.
38. Yang T, Xu X, Kernan T, Wu V, Colecraft HM (2010) Rem, a member of the RGK GTPases, inhibits recombinant CaV1.2 channels using multiple mechanisms that require distinct conformations of the GTPase. J Physiol 588: 1665–1681.
39. Correll RN, Pang C, Finlin BS, Dailey AM, Satin J, et al. (2007) Plasma membrane targeting is essential for Rem-mediated $Ca^{2+}$ channel inhibition. J Biol Chem 282: 28431–28440.
40. DeGeorge BR, Jr., Gao E, Boucher M, Vinge LE, Martini JS, et al. (2008) Targeted inhibition of cardiomyocyte Gi signaling enhances susceptibility to apoptotic cell death in response to ischemic stress. Circulation 117: 1378–1387.
41. Volkers M, Weidenhammer C, Herzog N, Qiu G, Spaich K, et al. (2011) The inotropic peptide betaARKct improves betaAR responsiveness in normal and failing cardiomyocytes through G(betagamma)-mediated L-type calcium current disinhibition. Circ Res 108: 27–39.
42. Albarran-Juarez J, Gilsbach R, Piekorz RP, Pexa K, Beetz N, et al. (2009) Modulation of $\alpha_2$-adrenoceptor functions by heterotrimeric $G\alpha_i$ protein isoforms. J Pharmacol Exp Ther 331: 35–44.
43. Jiang M, Spicher K, Boulay G, Martin-Requero A, Dye CA, et al. (2002) Mouse gene knockout and knockin strategies in application to α subunits of $G_i/G_o$ family of G proteins. Methods Enzymol 344: 277–298.
44. Rudolph U, Finegold MJ, Rich SS, Harriman GR, Srinivasan Y, et al. (1995) Ulcerative colitis and adenocarcinoma of the colon in $G\alpha_{i2}$-deficient mice. Nat Genet 10: 143–150.
45. Skokowa J, Ali SR, Felda O, Kumar V, Konrad S, et al. (2005) Macrophages induce the inflammatory response in the pulmonary Arthus reaction through $G\alpha_{i2}$ activation that controls C5aR and Fc receptor cooperation. J Immunol 174: 3041–3050.
46. Ruan H, Mitchell S, Vainoriene M, Lou Q, Xie LH, et al. (2007) $G_i$ $\alpha_1$-mediated cardiac electrophysiological remodeling and arrhythmia in hypertrophic cardiomyopathy. Circulation 116: 596–605.
47. Ikuno Y, Leong FL, Kazlauskas A (2000) Attenuation of experimental proliferative vitreoretinopathy by inhibiting the platelet-derived growth factor receptor. Invest Ophthalmol Vis Sci 41: 3107–3116.

## Author Contributions

Conceived and designed the experiments: SD SK RPP BN SH. Performed the experiments: SD SK FK CK. Analyzed the data: SD SK FK PH CK RPP J. Matthes J. Meszaros SH. Wrote the paper: SD PH J. Matthes RPP BN SH. Critical revisions of the manuscript: SD PH J. Matthes RPP BN SH.

48. Heubach JF, Trebess I, Wettwer E, Himmel HM, Michel MC, et al. (1999) L-type calcium current and contractility in ventricular myocytes from mice overexpressing the cardiac beta 2-adrenoceptor. Cardiovasc Res 42: 173–182.

49. Meszaros J, Coutinho JJ, Bryant SM, Ryder KO, Hart G (1997) L-type calcium current in catecholamine-induced cardiac hypertrophy in the rat. Exp Physiol 82: 71–83.